Lattice-distortion-mediated local jumps of hydrogen in niobium from diffuse neutron scattering

H. Dosch, F. Schmid,* P. Wiethoff, and J. Peisl
Sektion Physik der Universität München, D-8000 München 22, Germany
(Received 1 October 1991)

We reconsider the mobility of hydrogen in bcc metals, in particular H and D in Nb, and its influence on the coherent and incoherent quasielastic neutron and x-ray scattering. An approach to describe time-dependent lattice distortions around highly mobile protons is presented, using the frequency-dependent Green's function of the host lattice so that effects of the so-called quasielastic effects and resonances with host lattice phonons are included. We discuss within this formalism how noncubic components of the long-ranged displacement field can fade away in the presence of a high defect mobility and we demonstrate by a detailed calculation that the experimentally observed disappearance of the coherent quasielastic diffuse (x-ray and neutron) scattering in NbH_x (NbD_x) from these Fourier components of the displacement field points to an unusual, hitherto neglected rapid local diffusion process between adjacent tetrahedral sites with a short-time constant of $\tau_{loc} \simeq 10^{-13}-10^{-14}$ s. The consequences of such a diffusion mechanism on the incoherent quasielastic neutron scattering are discussed in detail. We show that the elastic incoherent structure factor of the interstitial proton exhibits, in addition to the usual Debye-Waller factor behavior, distinct oscillations as a function of the neutron momentum transfer. A neutron-scattering study of $NbH_{0.02}$ at various temperatures between room temperature and 573 K is presented. The experimental results of the elastic incoherent structure factor displays, after a proper correction for the proton Debye-Waller factor, a pronounced oscillatory behavior in the [100] and [111] direction as predicted for a rapid local diffusion on neighboring tetrahedral sites. It is shown that this property of the proton form factor is temperature dependent. We present measurements of the quasielastic broadening of the coherent diffuse neutron scattering from the time-dependent long-ranged displacement field ("Huang linewidth") and discuss further implications of our findings on the interpretation of structural and dynamical properties of H in Nb, as the local modes and the coherent diffuse neutron scattering from the lattice distortions around the local defect neighborhood.

I. INTRODUCTION

The location and dynamics of hydrogen dissolved in niobium and other bcc transition metals have been extensively studied now for about 20 years:[1] Neutron-scattering studies have provided detailed information on the location of the proton, its microscopic interstitial diffusion mechanism,[2,3] the host-lattice distortion around it, and its various vibrational modes. Recently, it has been pointed out[4,5] that, despite all these efforts, many features in all these microscopic properties of interstitial hydrogen remain unclear, such as the cubic symmetry of long-range lattice distortions,[6,7] the linewidth of incoherent quasielastic neutron scattering,[3] and the intrinsic energy width of the localized modes[8] (we do not repeat these arguments here and refer the reader to Ref. 5). A rigorous quantitative analysis of coherent diffuse neutron scattering from NbD_x disclosed a surprising detail.[5] By a detailed comparison of the observed diffuse scattering with various model calculations, it could be demonstrated that local distortions around the dissolved deuterium are incompatible with the assumption of a defect localized at one interstitial (tetrahedral) site. Instead, in order to reproduce the observed coherent-scattering pattern, one has to introduce local lattice distortions that are spread out over several neighboring interstitial sites. It was suggested that these rather unusual local lattice distortions are brought about by the mobility of the interstice.

In this paper we present theoretical and experimental studies of quasielastic coherent and quasielastic incoherent neutron scattering from NbD_x and NbH_x, respectively, which provide insight into these puzzling phenomena. We will show in what follows that local and long-ranged lattice distortions (as measured by coherent scattering) as well as the proton form factor (as obtained from elastic incoherent scattering) can naturally be explained by the assumption of a rapid local diffusion of interstitial hydrogen between adjacent tetrahedral sites. This idea will be developed below in several steps.

In Sec. II we present a theoretical approach to describe the lattice distortions due to highly mobile defects that shows rigorously that a rapid diffusion can destroy the long-ranged tetrahedral components of the defect-induced displacement field as it is observed.[7] A quantitative theoretical analysis of Huang diffuse scattering in NbD_x based on this approach shows that the intensity contributions from noncubic long-ranged host-lattice distortions disappear completely when the interstice performs a rapid local diffusion with a jumping frequency $\nu_{loc} \geq 10^{13}-10^{14}$ s^{-1}. We will give arguments that this rapid motion of the defect is localized in space involving only a few neighboring tetrahedral sites; thus it does not contribute to long-range diffusion. In Sec. III we calcu-

late incoherent neutron scattering from NbH_x, which is predicted to show interesting features in the presence of this rapid local-diffusion process. Experimental results from a quasielastic incoherent neutron-scattering study of NbH_x are presented in Sec. IV. They show unambiguously that the elastic incoherent structure factor ($S_{\rm inc}^{\rm el*}$) of the proton exhibits indeed an unusual phenomenon which is in contrast with all models assumed up to now: $S_{\rm inc}^{\rm el*}$ displays an oscillatory behavior in Q space, which is clear experimental evidence that the proton is delocalized. The proton delocalization occurs on a time scale which is much shorter than $\tau_{LR} \simeq 10^{-12}$ s associated with the conventional microscopic jumping mechanism which leads to long-ranged diffusion. It can thus be explained by a rapid localized motion of the proton between adjacent tetrahedral sites.

In Sec. V we discuss the consequences on the quasielastic broadening of coherent diffuse neutron scattering from the long-ranged displacement fields and show experimental results from NbD_x. Further implications on the interpretation of coherent quasielastic neutron scattering are discussed.

II. COHERENT DIFFUSE SCATTERING FROM TIME-DEPENDENT LATTICE DISTORTIONS

Dosch, Peisl, and Dorner[4,5] have pointed out in their analysis of local lattice distortions that the average relaxation time τ_R of the lattice displacement field is comparable to the time scale $\tau_{LR} \simeq 10^{-12}$ associated with the microscopic jump of the interstice. They argue that this leads to nonadiabatic lattice relaxations around several adjacent defect sites. Since neighboring tetrahedral sites have a different orientation of their individual distortion fields, this diffusion-mediated lattice-distortion field around several sites may have little or even no tetragonal component. Experimentally, it turns out that the long-range displacement field exhibits, within the experimental errors, no tetrahedral component, $F_{\rm expt} \equiv |B - A| \leq 0.1$ eV, where A and B denote the nonvanishing elements of the force dipole tensor

$$\underline{P} \equiv \begin{pmatrix} A & 0 & 0 \\ 0 & B & 0 \\ 0 & 0 & B \end{pmatrix}$$

associated with the tetrahedral interstice (see, e.g., Ref. 5). The most direct evidence for this rather unexpected property of long-ranged lattice distortions around the proton is the missing Huang diffuse scattering in the $\langle 1\bar{1}0 \rangle$ direction (so-called "angular" direction) close to "$(hh0)$"-type reciprocal-lattice vectors[7] (for an introductory discussion of Huang diffuse scattering from defects, we refer the reader to the articles by Trinkaus[9] and Dederichs[10]). We will show that the absence of this Huang diffuse scattering can be used as a very convenient criterion for an assessment of the underlying jumping frequency of the defect.

We derive the coherent diffuse neutron-scattering cross section due to time-dependent lattice distortions and start with the associate intermediate scattering function in continuum approximation,

$$I(\mathbf{q},t) = \frac{b_c^2}{V_{uc}^2} \langle (e^{i\mathbf{Q}\cdot\mathbf{u}})^2 \rangle \times \int d\mathbf{r} \int d\mathbf{r}' \, e^{i\mathbf{q}\cdot(\mathbf{r}-\mathbf{r}')} \times \langle [\mathbf{Q}\cdot\mathbf{u}(\mathbf{r}',t)][\mathbf{Q}\cdot\mathbf{u}(\mathbf{r},0)] \rangle \ , \quad (1)$$

where b_c is the coherent-scattering length of the host-lattice atoms, V_{uc} the volume of the host-lattice unit cell, $\langle (e^{i\mathbf{Q}\cdot\mathbf{u}})^2 \rangle$ the Debye-Waller factor, $\mathbf{q} \equiv \mathbf{Q} - \mathbf{G}_{hkl}$ ($\mathbf{G}_{hkl}$ = reciprocal-lattice vector), and

$$\mathbf{u}(\mathbf{r},t) = \mathbf{u}_{\rm ph}(\mathbf{r},t) + \mathbf{u}_{\rm def}(\mathbf{r},t) \quad (2)$$

the momentary displacement of the host-lattice atom at $\mathbf{r}$ from its average position. $\mathbf{u}_{\rm ph}(\mathbf{r},t)$ describes the phonon contribution and $\mathbf{u}_{\rm def}(\mathbf{r},t)$ the defect contribution, which is given in the continuum approximation by

$$\mathbf{u}_{\rm def}(\mathbf{r},t) = \int dt' \int d\mathbf{r}' \, g(\mathbf{r}-\mathbf{r}', t-t') \chi(\mathbf{r}',t') \ . \quad (3)$$

$\chi(\mathbf{r}',t')$ is the so-called Kanzaki-force density[11] exerted on the host lattice atoms at $\mathbf{r}'$, and

$$g(\mathbf{r},t) \equiv (2\pi)^{-1} \int d\omega \, e^{i\omega t} G(\mathbf{r},\omega) \quad (4)$$

is the dynamical lattice Green's function. Its Fourier transform $G(\mathbf{r},\omega)$ is defined as[12]

$$G(\mathbf{r},\omega) \equiv \int (2\pi)^{-3} \rho_0^{-1} \sum_i d\mathbf{q} \, e^{i\mathbf{q}\cdot\mathbf{r}} \frac{|\mathbf{e}_{i\mathbf{q}}\rangle\langle\mathbf{e}_{i\mathbf{q}}|}{\omega_{i\mathbf{q}}^2 - (\omega - i\eta_{i\mathbf{q}})^2} \ , \quad (5)$$

with $\mathbf{e}_{i\mathbf{q}}$ as the eigenvector of the phonon $(i,\mathbf{q})$ with eigenfrequency $\omega_{i\mathbf{q}}$ and phenomenological lifetime $\eta_{i\mathbf{q}}^{-1}$. ρ_0 is the mean density of the medium. The Kanzaki-force density $\chi(\mathbf{r},t)$ is related to the actual defect positions $\mathbf{r}_j(t)$ by

$$\chi(\mathbf{r},t) = \sum_j \psi_j(\mathbf{r} - \mathbf{r}_j(t)) \ , \quad (6)$$

where the label j denotes the (in our case) six nonequivalent tetrahedral sites $\mathbf{r}_j$ in the unit cell and $\psi_j(\mathbf{r}-\mathbf{r}_j(t))$ the Kanzaki force of a single defect on site $\mathbf{r}_j(t)$ acting on the host-lattice atom at $\mathbf{r}$. Since ψ_j is short ranged and $\int \psi_j(\mathbf{r}')d\mathbf{r}' = 0$, we get for small values of $\mathbf{q}$ ("Huang regime") the relation

$$\int d^3r \ \psi_j^{\mu}(\mathbf{r}) e^{i\mathbf{q}\cdot\mathbf{r}} \simeq i P_j^{\mu\nu} q^{\nu} \ , \quad (7)$$

with the well-known force dipole moment P (see Ref. 9) (μ,ν denote Cartesian coordinates). In the static case, P describes the long-ranged displacement field and has the form discussed above.

Consider now the situation of uncorrelated defects which perform rapid jumps between neighboring interstitial sites described by the transition probabilities $W_j^i(\mathbf{R},t)$ (=probability to find the proton at time t on site $\mathbf{r}_j$ of unit cell labeled $\mathbf{R}$, if it started at time $t=0$ from site $\mathbf{r}_i$ of the unit cell at the origin $\mathbf{0}$). The Fourier transform of the system of rate equations[1] becomes

$$W_j^i(\mathbf{q},t) = \sum_k e^{-\Gamma_k(\mathbf{q})|t|} U_{ik}(\mathbf{q}) [U_{kj}^{-1}(\mathbf{q})] \ , \quad (8)$$

where $\Gamma_k(\mathbf{q})$ is the eigenvalue and $U_{ik}(\mathbf{q})$ the eigenvector

of the transition matrix (we discuss this in more detail in Sec. III). One of the eigenvalues, Γ_1, is close to 0 for small values of $\mathbf{q}$, $\Gamma_1 \propto q^2$. If the diffusion process is spatially localized, $\Gamma_1=0$ holds exactly for all values of q. The other eigenvalues are of $O(\tau^{-1})$, where τ^{-1} is the jumping probability. It is quite instructive to consider the displacement-displacement correlation function $\xi^{\rm dis}_{\mu\nu}(\mathbf{r},t)\equiv\langle u^{\mu}_{\rm def}(\mathbf{r},t)u^{\nu}_{\rm def}(\mathbf{0},0)\rangle$, which enters implicitly the intermediary scattering function (1). Using Eqs. (5)–(8) we find that the Fourier transform reads, in the Huang regime ($q\rightarrow 0$),

$$\xi^{\rm dis}_{\mu\nu}(\mathbf{q},\omega)\propto\int dt\, e^{i\omega t}\sum_{i,j}W^{i}_{j}(\mathbf{q},t)(\underline{G}\,\underline{P}_i\mathbf{q})_{\mu}(\underline{G}^{*}\underline{P}_j\mathbf{q})_{\nu}$$
$$=\sum_k\frac{\Gamma_k}{\Gamma_k^2+\omega^2}\left[\underline{G}\sum_i U_{ik}\underline{P}_i\mathbf{q}\right]_{\mu}\times\left[\underline{G}^{*}\sum_j U_{kj}\underline{P}_j\mathbf{q}\right]_{\nu}. \quad (9)$$

$\xi^{\rm dis}_{\mu\nu}(\mathbf{q},\omega)$ exhibits a fundamental property which has to be appreciated by the reader: The term belonging to the smallest eigenvalue (=Lorentzian width) $\Gamma_1\simeq 0$ is associated with $\sum_i U_{i1}\underline{P}_i\simeq\sum_i\underline{P}_i$, thus with the *cubic part of the long-ranged displacement field.*[13] The other eigenvalues Γ_k ($k=2,3,\ldots$) are coupled with the *tetrahedral components of the displacement field,* which are accordingly strongly affected by the dynamics of the defect, since $\Gamma_k=O(\tau^{-1})$ for $k=2,3,\ldots$. This has, as we will see below, some crucial consequences for the diffuse scattering from the long-ranged displacement field. For the sake of argument we first discuss the somewhat simpler case of the diffusion on a Bravais lattice which is described by one eigenvalue $\Gamma(\mathbf{q})$; then the sum $\sum_k$ in Eq. (8) degenerates to $\exp[-\Gamma(\mathbf{q})|t|]$, and consequently the sum $\sum_k$ also drops out of Eq. (9). The intermediary scattering function (1) then simply is

$$I(\mathbf{q},t)=c_d N\frac{b_c^2}{V_{uc}^2}\langle(e^{i\mathbf{Q}\cdot\mathbf{u}})^2\rangle\times\int dt'\int dt''\,s(t')s(t'')e^{-\Gamma(\mathbf{q})|t'-t''|}, \quad (10)$$

with c_d as the defect concentration and

$$s(t)=(2\pi\rho_0)^{-1}\int d\omega\, e^{i\omega t}\sum_i\frac{(\mathbf{e}_{i\mathbf{q}}\cdot\mathbf{Q})(\mathbf{e}_{i\mathbf{q}}\cdot\underline{P}\mathbf{q})}{\omega_{i\mathbf{q}}^2-(\omega-i\eta_{i\mathbf{q}})^2}. \quad (11)$$

After its Fourier transformation, we obtain the scattering cross section of the Huang diffuse scattering (HDS) from time-dependent lattice distortions,

$$\left[\frac{d^2\sigma}{d\Omega\,d\omega}\right]^{\rm HDS}_{\rm coh}(\mathbf{Q};\mathbf{q},\omega)$$
$$=c_d N\frac{k_f}{k_i}\frac{b_c^2}{m_0^2}\langle(e^{i\mathbf{Q}\cdot\mathbf{u}})^2\rangle\pi^{-1}\frac{\Gamma(q)}{\Gamma^2+\omega^2}\times\left|\sum_i\frac{(\mathbf{e}_{i\mathbf{q}}\cdot\mathbf{Q})(\mathbf{e}_{i\mathbf{q}}\cdot\underline{P}\mathbf{q})}{\omega_{i\mathbf{q}}^2-(\omega+i\eta_{i\mathbf{q}})^2}\right|^2, \quad (12)$$

which contains in addition to the quasielastic broadening of the Huang diffuse scattering ("Lorentzian" term), which has recently been discussed by Gillan and Wolf,[14] another term ("phonon resonance" term) which accounts for the interaction of the defect diffusional modes with host-lattice phonons. In order to make the physical meaning of these two terms more transparent, we consider the generic function

$$\Theta(\mathbf{q},\omega)\equiv\frac{\Gamma}{\Gamma^2+\omega^2}\left|\frac{1}{\omega_{\mathbf{q}}^2-(\omega+i\eta)^2}\right|^2. \quad (13)$$

$\omega_{\mathbf{q}}$ plays the role of the phonon frequency associated with the reduced momentum transfer $\mathbf{q}$. Figure 1 shows $\Theta(\mathbf{q},\omega)$ versus ω for various values of $\Gamma/\omega_{\mathbf{q}}$ and for a fixed value $\eta\rightarrow 0$. We find a three-peak structure: The two appearing at $\omega=\pm\omega_{\mathbf{q}}$ originate from the relaxation dynamics of the lattice distortions taking place via phonon-absorption and -emission processes: At the reduced momentum $\mathbf{q}$, the associated Fourier components of the lattice distortions can relax through the host-lattice modes $\omega_{\mathbf{q}}$. In addition, a quasielastic intensity appears at $\omega=0$. In the static case this intensity is purely elastic and then conventionally called defect-induced Huang diffuse scattering. As we see from inspection of Fig. 1, its integrated intensity and width depends sensitively upon the actual value of $\Gamma/\omega_{\mathbf{q}}$: The short-dashed line illustrates the case $\Gamma/\omega_{\mathbf{q}}\ll 1$, thus the case of a defect with a low jumping frequency compared with the frequency of the relevant lattice vibrations: The small Lorentzian allows only for intensity as long as $\omega\le\Gamma\ll\omega_{\mathbf{q}}$; i.e., there is no interference of the diffusion process with the host-lattice vibrations. In other words, the lattice follows the defect motion adiabatically, and Eq. (12) reduces to the Gillan-Wolf form[14]

$$\left[\frac{d^2\sigma}{d\Omega\,d\omega}\right]_{\rm coh}(\mathbf{Q};\mathbf{q},\omega)\propto\frac{k_f}{k_i}\frac{\Gamma(\mathbf{q})}{\Gamma^2(\mathbf{q})+\omega^2}\left[\frac{d\sigma}{d\Omega}\right]^{\rm el}_{\rm coh}(\mathbf{Q};\mathbf{q}), \quad (14)$$

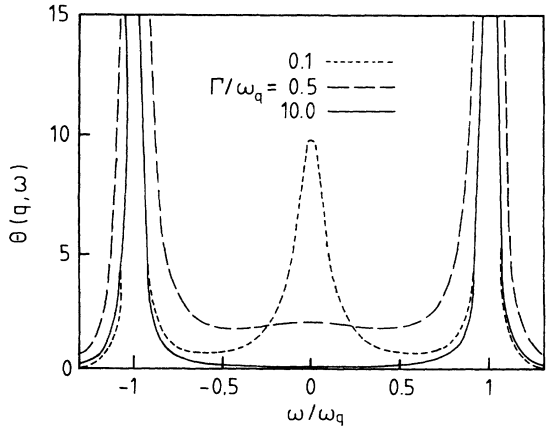

FIG. 1. Function $\Theta(\mathbf{q},\omega)$ vs $\omega/\omega_{\mathbf{q}}$ for various values of $\Gamma/\omega_{\mathbf{q}}$.

where $(d\sigma/d\Omega)^{el}_{coh}$ is the coherent elastic diffuse scattering due to a "frozen" defect [the associated structure factor will be given below in Eq. (32)]. In this case the mobility of the defect merely leads to a quasielastic broadening of the Huang diffuse scattering. More exciting, however, is the case when $\Gamma/\omega_q \simeq 1$ (dashed and short-dashed lines), since here the associated phonon becomes resonant with the host-lattice distortions of the mobile defect. Now the Huang diffuse intensity decays significantly, a phenomenon that is due to the fact that the host lattice around the interstice can no longer relax completely. Finally, in the extreme case, where $\Gamma/\omega_q \gg 1$ (solid line in Fig. 1), no long-ranged lattice displacements are allowed anymore and the associated Huang diffuse scattering has fully disappeared. We conclude from these fundamental properties of $\Theta(\mathbf{q},\omega)$ that components of the long-ranged displacements field may disappear when the Lorentzian width $\Gamma(\mathbf{q})$ exceeds a certain critical value.

With this information we now turn to the case of hydrogen in bcc metals, in particular to NbH_x. As an obvious complication, we have to consider now that the diffusion takes place on a non-Bravais lattice, which leads to a more involved expression; however, the basic features of the scattering cross section (12) and its generic function $\theta(\mathbf{q},\omega)$(13) remain: Inserting (9) into the intermediary scattering function (1) and performing the Fourier transformation, the Huang-diffuse-scattering cross section then reads

$$\left[\frac{d^2\sigma}{d\Omega\, d\omega}\right]^{HDS}_{coh}(\mathbf{Q};\mathbf{q},\omega)=c_d N\frac{k_f}{k_i}\frac{b_c^2}{m_0^2}\langle(e^{i\mathbf{Q}\cdot\mathbf{u}})^2\rangle\frac{1}{\pi}\sum_p\frac{\Gamma_p(\mathbf{q})}{\Gamma_p^2+\omega^2}\left[\sum_{i,k}w_k U_{kp}\frac{(\mathbf{e}_{i\mathbf{q}}\cdot\mathbf{Q})(\mathbf{e}_{i\mathbf{q}}\cdot\underline{P}_k\mathbf{q})}{\omega_{i\mathbf{q}}^2-(\omega-i\eta_{i\mathbf{q}})^2}\right]\times\left[\sum_{j,l}(U^{-1})_{pl}\frac{(\mathbf{e}_{j\mathbf{q}}\cdot\mathbf{Q})(\mathbf{e}_{j\mathbf{q}}\cdot\underline{P}_l\mathbf{q})}{\omega_{j\mathbf{q}}^2-(\omega+i\eta_{j\mathbf{q}})^2}\right], \tag{15}$$

where w_k is the occupation probability of the defect site k ($k=1,2,\ldots,6$ in the case of tetrahedral sites in bcc lattices). Associated with the tetrahedral symmetry of the frozen proton, the force dipole moment $\underline{P}_k$ has now noncubic symmetry. We already mentioned above that its cubic part is coupled to small width Γ_1, i.e., generally $\Gamma_1/\omega_q \ll 1$ holds and the associated Huang-diffuse-scattering contribution is expected to "survive" when the proton performs jumps on the interstitial lattice. Since, on the other hand, the noncubic components of the long-ranged displacement field are coupled to $\Gamma_{2,3,\ldots}=O(\tau^{-1})$, the presence of these components should crucially depend on the mobility of the defect. This turns out to be the case: We describe the frozen proton by a noncubic force dipole moment

$$\underline{P}=P_0\begin{pmatrix}1&0&0\\0&2&0\\0&0&2\end{pmatrix}$$

associated with the tetrahedral site in bcc lattices using $P_0=2$ eV according to the observed value $\mathrm{tr}\underline{P}=10$ eV in Nb.[7] Note that we assumed here that the lattice distortions of the "frozen" proton preserve the full tetrahedral symmetry of the tetrahedral site, $F_0=|A-B|=2$ eV.[5] The Nb host-lattice response is given by the dynamical matrix $\underline{D}(\mathbf{q})$, which assumes, in the Huang regime ($q\to 0$), the asymptotic form

$$\underline{D}(\mathbf{q})=\begin{pmatrix}c_{44}+(c_{11}-c_{44})r_1r_1 & (c_{44}+c_{12})r_1r_2 & (c_{44}+c_{12})r_1r_3\\ (c_{44}+c_{12})r_1r_2 & c_{44}+(c_{11}-c_{44})r_2r_2 & (c_{44}+c_{12})r_2r_3\\ (c_{44}+c_{12})r_1r_3 & (c_{44}+c_{12})r_2r_3 & c_{44}+(c_{11}-c_{44})r_3r_3\end{pmatrix}, \tag{16}$$

with $c_{\mu\nu}$ as the elastic constants of Nb (Ref. 15) and $r_\mu\equiv q_\mu/q$. Remember that the phonon frequencies $\omega_{i\mathbf{q}}$ are the eigenvalues of $\underline{D}(\mathbf{q})$.

In Fig. 2 we show the coherent diffuse neutron-scattering cross section versus energy transfer in NbD_x as calculated from Eqs. (15) and (16) for $\mathbf{q}=q_0(1,-1,0)$, $q_0=0.05$, and $G_{hkl}=(h,h,0)$ chosen such that this coherent quasielastic scattering is solely due to long-ranged *tetrahedral* Fourier components of the displacement field (see Ref. 9). The proton jumping frequency ranges from $\nu=10^{11}$ to 10^{13} s^{-1}. Of course, we again find the three-peak structure as already discussed above, whereby now ω_q is associated with the transverse phonon $\omega_T(\mathbf{q})\approx 0.5\times 10^{12}$ Hz in Nb [as deduced from Eq. (16)]. The interesting result from this calculation is that the tetrahedral quasielastic component smears out and decays considerably, when ν exceeds 10^{11} s^{-1} (in apparent agreement with the estimation by Dosch, Peisl, and Dorner[4,5] using the small-polaron theory[16]), and eventually disappears for $\nu\geq 10^{13}$ s^{-1}. This shows that the long-ranged Nb host-lattice displacements depend sensitively upon the mobility of the dissolved proton. The key question is now, which tetragonality $F(q_0,\nu)$ for a given value of $\mathbf{q}_0$ could be observed within our approach in the x-ray Huang-diffuse-scattering experiment described by Metzger, Peisl, and Wanagel.[7] We note that this diffuse x-ray intensity is obtained in the actual experiment from NbH_x after subtracting the x-ray scattering from the pure Nb reference crystal (mainly one-phonon scattering). Within our approach this diffuse x-ray intensity is

given by[17]

$$\left[\frac{d\sigma}{d\Omega}\right]_{\text{coh}}^{\text{HDS}} = \sum_p \left[\sum_{i,k} w_k U_{kp} \frac{(\mathbf{e}_{iq}\cdot\mathbf{Q})(\mathbf{e}_{iq}\cdot\underline{P}_k\mathbf{q})}{\Gamma_p^2+\omega_{iq}^2}\right] \times \left[\sum_{j,l}(U^{-1})_{pl}\frac{(\mathbf{e}_{jq}\cdot\mathbf{Q})(\mathbf{e}_{jq}\cdot\underline{P}_l\mathbf{q})}{\omega_{iq}^2}\right], \tag{17}$$

which can be used now in a straightforward way to calculate the observable tetragonality $F(q_0,\nu)$ (in units of eV) as a function of the jumping frequency ν of the proton. The result of such a calculation is shown in Fig. 3(a) for various values of q_0 in the $\mathbf{q}=q_0(1,-1,0)$ direction of the $(h,h,0)$ Brillouin zone. We conclude that $F(q_0,\nu)$ remains virtually unaffected, $F(q_0,\nu)=F_0=2$ eV, as long as the jumping frequency of the proton is less than $\nu\simeq 5\times 10^{11}$ s^{-1}; however, it decays dramatically when ν becomes larger than 10^{12} s^{-1}. According to our theoretical approach, the disappearance of the Huang diffuse scattering naturally depends upon the value q_0; the larger q_0 is, the more shifted to higher ν is the decrease of the tetragonality F. This behavior has a very intuitive reason: At small q_0 the scattering experiment is sensitive to tetrahedral displacement components far away from the defect. These long-ranged Fourier components of the displacement field follow the defect motion only slowly and, accordingly, fade away already at relatively small values of ν. For large q_0 we are testing tetrahedral distortions closer to the defect that can react rather quickly via high-frequency phonons and, thus, may survive up to some higher values of ν. The remarkable conclusion according to Fig. 3(a) now is that one needs a jumping frequency of

$$\nu_{\text{loc}}^{*}\simeq 8\times 10^{13}\ \text{s}^{-1}, \tag{18}$$

in order to render $F\simeq F_{\text{expt}}<0.1$ eV for $q_{\text{expt}}<0.1$.[7] Thus, assuming that the lattice distortions around the

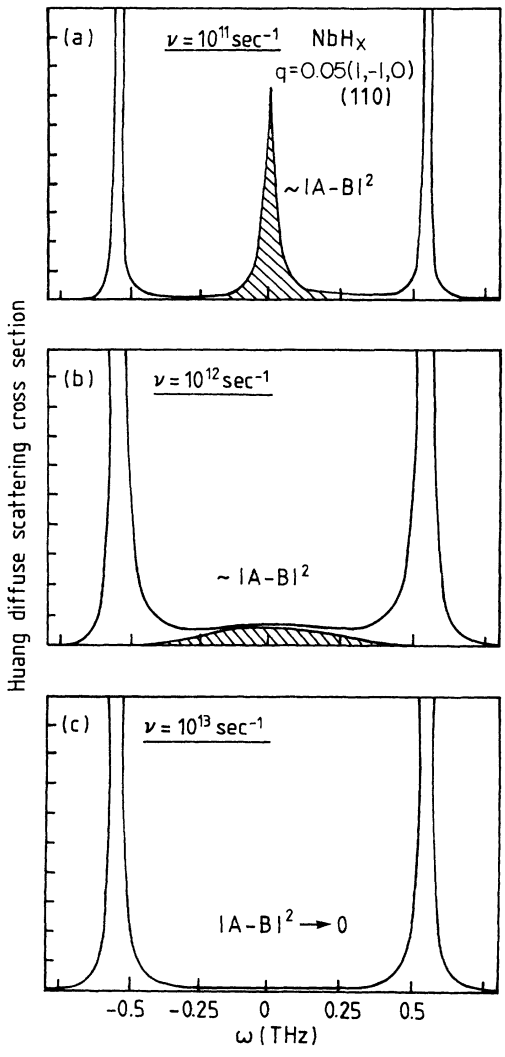

FIG. 2. Huang diffuse neutron scattering from $NbH_x(NbD_x)$: (a) Energy distribution of the diffuse scattering at $\mathbf{q}=\mathbf{Q}-G_{hh0}=q_0(1,1,0)$ and $q_0=0.05$ as a function of ω for different values of the defect jumping frequency (a) $\nu=10^{11}$ s^{-1}, (b) $\nu=10^{12}$ s^{-1}, and (c) $\nu=10^{13}$ s^{-1}. The hatched area is the Huang diffuse intensity which is proportional to the squared tetragonality $F^2=|A-B|^2$ (for explanation, see main text).

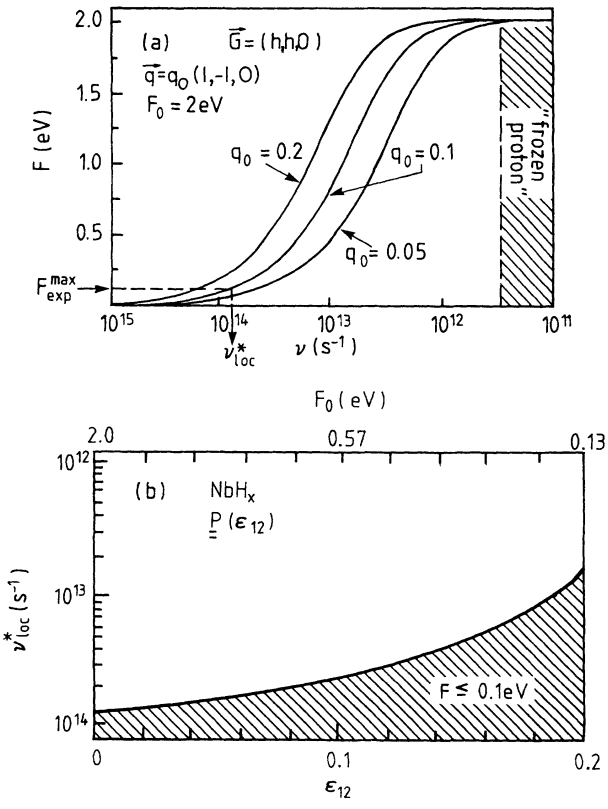

FIG. 3. (a) Predicted tetragonality F of the long-ranged displacement field vs jumping frequency of the defect as deduced from Huang diffuse scattering at $q_0=0.05,0.1,0.2$. The experimental upper limit $F_{\text{expt}}^{\max}(q_0=0.1)=0.1$ eV (Ref. 7) and the associated ν_{loc}^{*} are indicated. (b) Critical jumping frequency ν_{loc}^{*} of the interstitial proton in Nb to achieve $F(\nu_{\text{loc}}^{*})=0.1$ eV vs the parameter ϵ_{12} or vs frozen tetragonality F_0 (upper scale).

frozen proton preserve the full tetrahedral symmetry F_0, $\nu^*_{\rm loc}$ should be almost two orders of magnitude larger than the jumping frequency responsible for the long-range diffusion. If the "frozen" tetragonality F_0 is somewhat reduced, the necessary critical value $\nu^*_{\rm loc}$ to destroy it will accordingly be smaller. To estimate this effect we describe the force dipole tensor of the frozen proton by Kanzaki forces on nearest and next-nearest neighbors and arrive at the expression[5]

$$\underline{P}(\epsilon_{12})=P_0\left\{\begin{bmatrix}1&0&0\\0&2&0\\0&0&2\end{bmatrix}+(\tfrac{5}{13})^{1/2}\epsilon_{12}\begin{bmatrix}9&0&0\\0&2&0\\0&0&2\end{bmatrix}\right\}, \tag{19}$$

where $\epsilon_{12}\equiv\psi_2/\psi_1$ is ratio of the radial forces ψ_2 and ψ_1 on the second- and first-neighbor shell around the frozen proton. (When the absence of noncubic long-ranged displacement components was detected, it was originally suggested[6] that $\epsilon_{12}=0.23$, which would indeed render $\underline{P}$ cubic for the immobile proton. However, the analysis of the coherent diffuse neutron scattering from the local defect neighborhood showed quite clearly[5] that this model is incorrect; see also final remarks.) In Fig. 3(b) we show the result of the calculation of $\nu^*_{\rm loc}$ as a function of ϵ_{12} between $\epsilon_{12}=0$ associated with the full frozen tetragonality and the large value $\epsilon_{12}=0.2$ which creates, as mentioned, already wrong local distortions. We now find that the critical jumping frequency $\nu^*_{\rm loc}$, which renders $\underline{P}(\epsilon_{12})$ cubic, has to be in the range

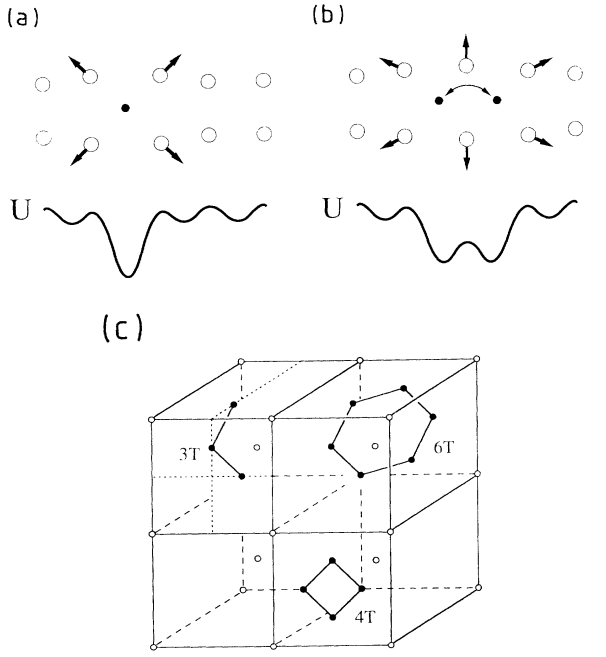

FIG. 4. (a) and (b) Schematic picture of the host lattice (open circles) distorted by the interstitial defect and interstitial potential (the short arrows indicate the displacements of the host lattice atoms) (a) for a (quasi)frozen defect and (b) for a highly mobile defect jumping at a high rate between two neighboring sites (see text). (c) Some possible configurations of a rapid local diffusion.

$$\nu^*_{\rm loc}\simeq(1-8)\times10^{13}\ {\rm s}^{-1}, \tag{20}$$

depending on the assumptions on ϵ_{12}. Quite clearly, this high value of the critical jumping frequency $\nu^*_{\rm loc}$ would be in severe contradiction to the macroscopic diffusion constant of the interstitial proton,[2] unless one introduces a strong correlation ("memory effect") between these ultrafast jumps. Such correlations can be mediated by the unusual local lattice distortions as reported by Dosch, Peisl, and Dorner.[4,5] The situation is illustrated in simple terms in Fig. 4: In Fig. 4(a) we consider the conventional low jump rate where the interstitial defect distorts the surrounding lattice, thereby lowering the potential energy on the occupied interstice. In Fig. 4(b) we show the case of such a high jump rate that the lattice is no longer able to follow the individual jumps and is consequently distorted around an entire configuration of tetrahedral sites (as found experimentally[5]). Since the potential within this configuration is lowered, the proton is kept within the distorted region for a series of jumps. Thus, during this time, the jumps are highly correlated and practically do not contribute to the long-range diffusion. *Long-range diffusion* then results from the thermally activated motion of these entire configurations. Some conceivable configurations consisting of three, four, and six tetrahedral sites ($3T,4T,6T$) are depicted in Fig. 4(c). We comment on possible local-diffusion mechanisms in the final remark at the end of this article. As we shall see, the features of $S^{\rm el}_{\rm inc}$, which is considered in the experimental study described in Sec. IV, are independent of the details of the microscopic diffusion mechanism; therefore we subsequently treat the proton, for the sake of argument, as a classically diffusing particle.

III. LOCAL RAPID DIFFUSION AND INCOHERENT NEUTRON SCATTERING

Since in a neutron-scattering experiment on NbH_x the incoherent scattering is almost exclusively due to the hydrogen [$\sigma_{\rm inc}({\rm H})=80$ barn $\sigma_{\rm inc}({\rm Nb})=0.0024$ barn], the incoherent structure factor in this system is the Fourier-transformed self-correlation function of the interstitial proton,[18]

$$S_{\rm inc}(\mathbf{Q},\omega)=\frac{1}{2\pi\hbar}\int d\mathbf{r}\int dt\, G_s(\mathbf{r},t)e^{i(\mathbf{Q}\cdot\mathbf{r}-\omega t)}, \tag{21}$$

where

$$G_s(\mathbf{r},t)=\frac{1}{N}\sum_j\int d\mathbf{r}'\langle\delta(\mathbf{r}'-\mathbf{r}_j(0))\delta(\mathbf{r}'+\mathbf{r}-\mathbf{r}_j(t))\rangle \tag{22}$$

is the self-correlation function, $\mathbf{r}_j(t)$ the Heisenberg operator[19] of the jth proton, and $\langle\cdots\rangle$ the thermal average expectation value of the operator. Thus

$$S_{\rm inc}(\mathbf{Q},\omega)=\frac{1}{2\pi\hbar N}\int e^{-i\omega t}dt\sum_j\langle e^{-i\mathbf{Q}\cdot\mathbf{r}_j(0)}e^{i\mathbf{Q}\cdot\mathbf{r}_j(t)}\rangle. \tag{23}$$

By way of example we consider a proton performing random jumps on a $4T$ ring with a mean time of stay, τ, on one tetrahedral site, the generalization to other

configurations is straightforward: Let $W_{ij}(t)$ be the probability for a proton to be at site $\mathbf{r}_j$ at time t, if it has started at site $\mathbf{r}_i$. Note that $W_{ij}(t)$ corresponds to the correlation function $G_s(\mathbf{r}_j-\mathbf{r}_i, t)$ [Eq. (22)]. By solving a system of rate equations of the form

$$\frac{d}{dt}W_{11}(t)=-\frac{1}{\tau}W_{11}(t)+\frac{1}{2\tau}[W_{12}(t)+W_{14}(t)] , \tag{24}$$

we arrive at the solution

$$W_{ij}(t)=\sum_{k=1}^{4} S_{jk}(\underline{S}^{-1})_{ki}e^{-\Gamma_k|t|} , \tag{25}$$

where $\underline{S}$ is the matrix of eigenvectors belonging to the system of rate equations and Γ_k are the corresponding eigenvalues, $\Gamma_1=0$, $\Gamma_2=\Gamma_3=\tau^{-1}$, $\Gamma_4=2\tau^{-1}$. We calculate the intermediary scattering function

$$I(Q)\equiv\langle e^{-i\mathbf{Q}\cdot\mathbf{r}_j(0)}e^{i\mathbf{Q}\cdot\mathbf{r}_i(t)}\rangle$$
$$=\frac{1}{4}\sum_{i,j=1}^{4} W_{ij}(t)e^{i\mathbf{Q}\cdot(\mathbf{r}_j-\mathbf{r}_i)} , \tag{26}$$

and after its Fourier transformation and after averaging over all different orientations $\underline{P}$, we obtain the structure factor

$$S_{\mathrm{inc}}(\mathbf{Q},\omega)$$
$$=\sum_{p}\sum_{k=1}^{4}\frac{1}{2\pi\hbar}\frac{1}{12}\left[\frac{2}{\pi}\right]^{1/2}\sum_{i,j}S_{jk}(\underline{S}^{-1})_{ki}\times e^{i\mathbf{Q}\cdot(\mathbf{r}_j^p-\mathbf{r}_i^p)}\frac{\Gamma_k}{\omega^2+\Gamma_k^2} . \tag{27}$$

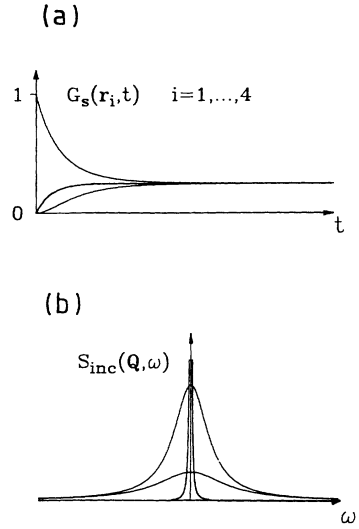

FIG. 5. (a) Self-correlation function $G_s(r_i,t)$ $(i=1,2,3,4)$ for rapid local diffusion within the $4T$ configuration (three inequivalent sites relative to the site occupied at time 0). (b) Associated incoherent structure factor (superposition of two Lorentzians and an elastic line). The purely elastic line indicates that no long-ranged diffusion occurs.

For a given $\mathbf{Q}$ the spectrum is a superposition of Lorentzians of widths Γ_k $(k=2,3,4)$ and an elastic line $(\Gamma_1=0)$. Since $\tau_{\mathrm{loc}}\simeq 10^{-14}$, the Lorentzians are expected to be very broad (20 meV or more). Figure 5 shows the self-correlation function and structure factor for rapid local diffusion on a $4T$ ring.

The integrated intensities of the Lorentzians and (quasi)elastic line (Γ_1) vary in $\mathbf{Q}$ space. The integrated quasielastic intensity is described by the elastic incoherent structure factor $S_{\mathrm{inc}}^{\mathrm{el}*}(\mathbf{Q})$, which will be defined below. In Fig. 6 the different incoherent intensities as calculated from (27) are plotted versus $\mathbf{Q}$ in the $\langle 001\rangle$ direction. We want to note that all intensity contributions exhibit the periodicity of the interstitial lattice and satisfy, of course, the well-known sum rule

$$\int_{-\infty}^{\infty} S_{\mathrm{inc}}(\mathbf{Q},\omega)d\omega=1 . \tag{28}$$

By splitting up the time-independent self-correlation function, the incoherent structure factor reads

$$S_{\mathrm{inc}}(\mathbf{Q},\omega)=\frac{1}{2\pi\hbar}\int\int e^{i(\mathbf{Q}\cdot\mathbf{r}-\omega t)}[\tilde{G}_s(\mathbf{r},t)+G_s(\mathbf{r},\infty)]d\mathbf{r}\,dt$$
$$\equiv S_{\mathrm{inc}}^{\mathrm{inel}}(\mathbf{Q},\omega)+S_{\mathrm{inc}}^{\mathrm{el}*}(\mathbf{Q})\delta(\omega) , \tag{29}$$

where $\tilde{G}_s(\mathbf{r},t)$ decays to zero as $|t|\to\infty$ and the elastic incoherent structure factor $S_{\mathrm{inc}}^{\mathrm{el}*}(\mathbf{Q})$ is given by the Fourier transform of the average distribution $G_s(\mathbf{r},\infty)$,

$$S_{\mathrm{inc}}^{\mathrm{el}*}(\mathbf{Q})=\int e^{i\mathbf{Q}\cdot\mathbf{r}}G_s(\mathbf{r},\infty)d\mathbf{r} . \tag{30}$$

In the following we consider the reciprocal plane determined by the (110) and (001) directions, which was also used in the neutron-scattering study on NbH_x described in Sec. IV. In Fig. 7(a), $S_{\mathrm{inc}}^{\mathrm{el}*}(\mathbf{Q})$ is illustrated for the case, where the proton performs rapid jumps between three adjacent sites ($3T$ configuration). $S_{\mathrm{inc}}^{\mathrm{el}*}(\mathbf{Q})$ is then the Fourier transform of the $3T$ configuration averaged over all possible orientations in the lattice and shows characteristic oscillations. $S_{\mathrm{inc}}^{\mathrm{el}*}(\mathbf{Q})$ for other local-diffusion paths between tetrahedral interstices looks quite similar, since it has the same interstitial symmetry. It differs mainly in the form and number of oscillations between the maxima. Figure 7(b) depicts, by way of example, the

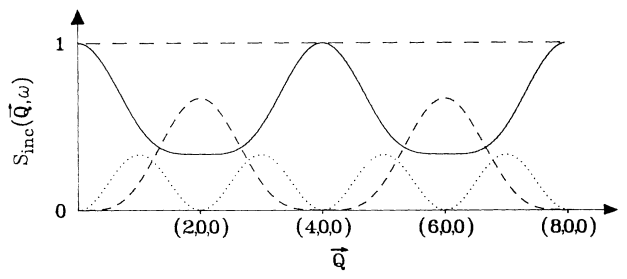

FIG. 6. Contributions to the incoherent structure factor associated with the $4T$ diffusion in the $\langle 100\rangle$ direction: The solid line shows the elastic line $(\Gamma_1=0)$, the dashed line the Lorentzian with $\Gamma_2=1/\tau$, and the dotted line the Lorentzian with $\Gamma_3=1/2\tau$. Note that the sum of all three contributions is equal to 1 independent of $\mathbf{Q}$ [sum rule Eq. (28)].

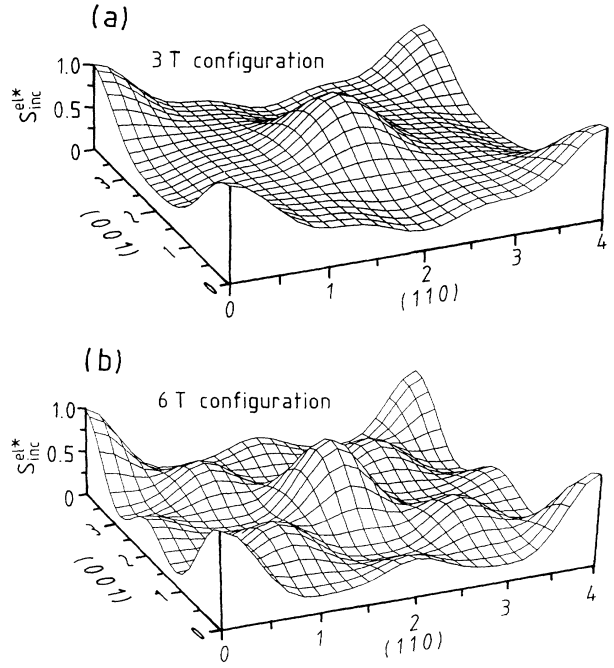

FIG. 7. Elastic incoherent structure factor $S_{\rm inc}^{\rm el*}$ for rapid local diffusion (a) on a $3T$ configuration and (b) on a $6T$ ring.

case where the proton is delocalized on a $6T$ ring. So far, we have tacitly neglected long-range diffusion, local modes, and band modes of the proton. Their effects on the elastic incoherent-scattering function $S_{\rm inc}^{\rm el*}(\mathbf{Q})$ [Eq. (30)], however, are accounted for in a straightforward way: The long-range diffusion results in the standard quasielastic broadening of the elastic line, denoted $S_{\rm inc}^{\rm el*}(\mathbf{Q},\omega)$. By integration over this quasielastic broadening, we recover again $S_{\rm inc}^{\rm el*}$, $S_{\rm inc}^{\rm el*}(\mathbf{Q})=\int_{\rm qe} S_{\rm inc}^{\rm qe*}(\mathbf{Q},\omega)d\omega$. The vibratory motion causes a Debye-Waller factor attenuation of $S_{\rm inc}^{\rm el*}(\mathbf{Q})$,

$$S_{\rm inc}^{\rm el}(\mathbf{Q})=e^{-Q^2\langle u_{\rm H}^2\rangle}S_{\rm inc}^{\rm el*}(\mathbf{Q},\omega)\ , \tag{31}$$

where $\langle u_{\rm H}^2\rangle$ is the mean-square amplitude of the localized modes and band modes of the proton.[20] Thus, to include band and localized modes, we multiply $S_{\rm inc}^{\rm el*}(\mathbf{Q})$ by the Debye-Waller factor $\exp(-\mathbf{Q}^2\langle u_{\rm H}^2\rangle)$ of Eq. (31) and obtain $S_{\rm inc}^{\rm el}(\mathbf{Q})$ for the $3T$ configuration [Fig. 8(a)] and for the $6T$ ring [Fig. 8(b)].

We conclude that the proposed rapid local diffusion should give rise to a periodically *oscillating* incoherent elastic structure factor $S_{\rm inc}^{\rm el*}(\mathbf{Q})$, which should be readily detectable in a neutron-scattering experiment after correction for the proton Debye-Waller factor. This scattering study will be described next.

IV. EXPERIMENTAL DETERMINATION OF $S_{\rm inc}^{\rm el}$ IN $NbH_{0.02}$

This experiment was performed at the triple-axis spectrometer IN3 at the Institut Laue-Langevin, Grenoble. We used a cylindrical ⟨110⟩ single crystal of niobium ($h=4$ cm, $r=0.5$ cm), which was degassed and cleaned and afterwards loaded with 2 at. % hydrogen by the standard procedure.[21] We measured $S_{\rm inc}^{\rm el}(\mathbf{Q})$ at three different temperatures: 295, 423, and 572 K, for this the sample was mounted in an evacuated furnace which also removed unwanted air scattering at small scattering angles. To determine $S_{\rm inc}^{\rm el}(\mathbf{Q})$ we took constant-Q scans across the quasielastic line at about 20 different $\mathbf{Q}$ values along each of the directions ⟨001⟩, ⟨110⟩, and ⟨111⟩. Figure 9 shows the associated reciprocal plane with the intensity contours deduced from Fig. 7(a). Figure 9 also includes the Brillouin-zone scheme of the bcc host lattice

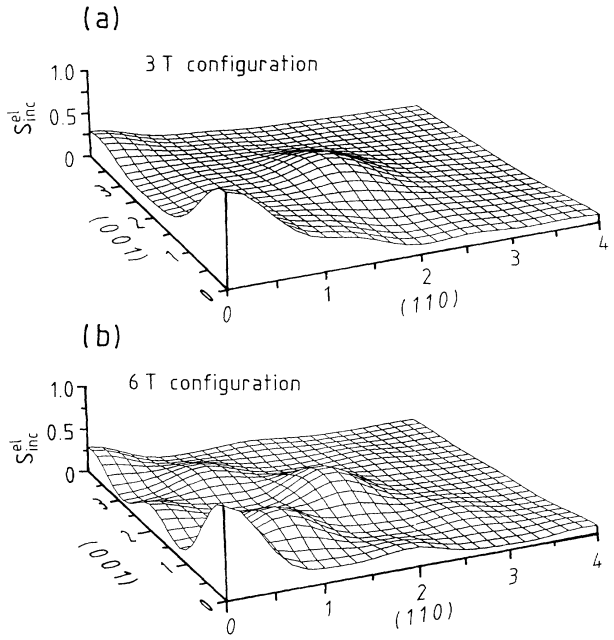

FIG. 8. Elastic incoherent structure factor $S_{\rm inc}^{\rm el}$ (including the Debye-Waller factor) for rapid local diffusion (a) on a $3T$ configuration and (b) on a $6T$ ring.

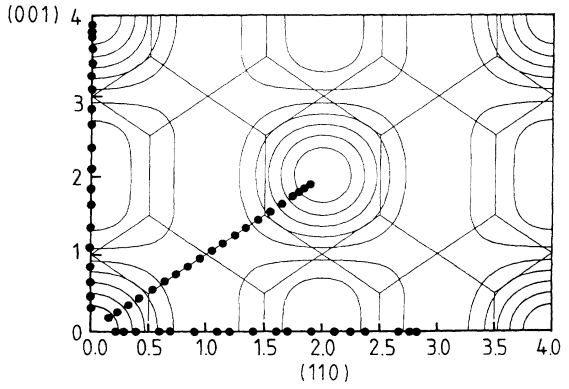

FIG. 9. Reciprocal plane showing the points where the incoherent elastic structure factor of $NbH_{0.02}$ has been measured (solid circles). Also shown are the intensity contours of the calculated $S_{\rm inc}^{\rm el*}$ [from Fig. 7(a)] and the Brillouin-zone scheme of the Nb host lattice.

and those points where the incoherent quasielastic line was determined (solid circles): In the ⟨001⟩ direction we covered a momentum transfer up to $\mathbf{Q}_{max}=(0,0,4)$, thus the whole tetrahedral Brillouin zone, in the ⟨111⟩ direction up to $\mathbf{Q}_{max}=(2,2,2)$; by this, one ranges one full period of the oscillating quantity $S_{inc}^{el*}(\mathbf{Q})$ [see also Fig. 7(a)]. In the ⟨110⟩ direction the momentum range was limited by the energy of the incoming neutrons to the maximum momentum transfer of $\mathbf{Q}=(3,3,0)$. The scans were performed in the constant-k_f mode with $k_f=2.662$ Å^{-1} for small $|\mathbf{Q}|$ and $k_f=4.4$ Å^{-1} for large $|\mathbf{Q}|$, using PG(002) and Cu(111) monochromators, respectively, and a PG(002) analyzer. The three collimators had a divergence of 60 min each.

Figure 10 shows a typical spectrum obtained by a constant-Q scan at $\mathbf{Q}=0.35(1,1,1)$ and $T=573$ K. The fitted curve is a Lorentzian[22] convoluted with the instrumental resolution ($\Delta E=0.98$ meV for $k_f=2.662$ Å^{-1}, $\Delta E=3.75$ meV for $k_f=4.4$ Å^{-1}). The deduced integrated intensity $S_{inc}^{el}(\mathbf{Q})$ was calibrated into an absolute scale by two different methods: The scans taken with $k_f=4.4$ Å^{-1} (large momentum transfer) were calibrated by reference to measured phonon intensities.[5] The intensities obtained with $k_f=2.662$ Å^{-1} (small momentum transfer) were extrapolated to $Q=0$, where $S_{inc}^{el}(\mathbf{Q})=S_{inc}^{el*}(\mathbf{Q})=1$ (i.e., independent of any Debye-Waller factor); the extrapolated number of counts at $Q=0$ was used as the standard of calibration. Both methods yielded within the experimental error the same absolute values for $S_{inc}^{el}(\mathbf{Q})$ in the range of medium momentum transfer, where scans were taken with both k_f values. In Fig. 11(a) the experimental result for $S_{inc}^{el}(\mathbf{Q})$ is shown along the ⟨001⟩ direction in absolute (dimensionless) units. As a by-product, the fitting yielded the width $\Gamma(\mathbf{Q})$ of $S_{inc}^{el}(\mathbf{Q})$ versus $\mathbf{Q}$ in the [110] and [111] direction (Fig. 12). Even though the error bars are large, as our energy resolution was not adjusted to a study of the linewidth, the observed quasielastic broadening shows values in the expected energy range and with the periodicity characteristic for interstitial long-range diffusion on tetrahedral sites. We considered these widths as a reliability check of our fitting procedure, which apparently worked very well.

The raw data shown in Fig. 11(a) have to be corrected for the defect-induced distortion scattering which is always present. As discussed in great detail in Ref. 5, the distortion scattering appears as a coherent elastic background, which is generally small compared to the strong incoherent scattering from the proton except near the Bragg reflections (which is then called Huang diffuse scattering as discussed in Sec. II). The associated structure factor is given by[5]

$$S_{coh}^{el}(\mathbf{Q})=\left\langle \left| b_c^{H}\exp(-\tfrac{1}{2}Q^2\langle u_H^2\rangle) + b_c^{Nb}\exp(-\tfrac{1}{2}Q^2\langle u_{Nb}{}^2\rangle) \times \sum_n (e^{i\mathbf{Q}\cdot\mathbf{u}_n^p}-1)(e^{i\mathbf{Q}\cdot\mathbf{r}_n^p}) \right|^2 \right\rangle_p . \quad (32)$$

$\langle u_{Nb}{}^2\rangle/T=1.92\times10^{-5}$ Å^2/K is the mean-square thermal displacement per degree kelvin of Nb in the high-temperature approximation and $\langle\cdots\rangle_p$ the average over all defect sites $\mathbf{r}_p$. The sum $\sum_n$ runs over all host lattice atoms on sites $\mathbf{R}_n$ with a static displacement $\mathbf{u}_n^p$ due to the defect at site $\mathbf{r}_p$. b_c^H and b_c^{Nb} denote the coherent-scattering lengths of hydrogen and niobium, respectively, and $\mathbf{r}_n^p\equiv\mathbf{R}_n-\mathbf{r}_p$. The distortion scattering

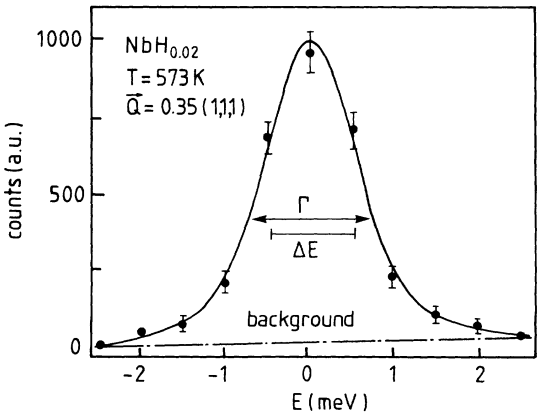

FIG. 10. Typical quasielastic neutron spectrum as obtained from $NbH_{0.02}$ at $\mathbf{Q}=0.35(1,1,1)$ and $T=573$ K. The fit is a Lorentzian convoluted with the instrumental energy resolution.

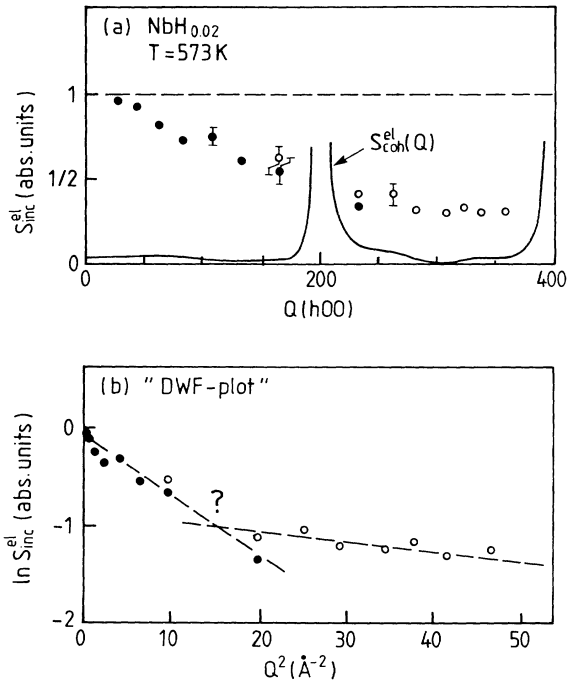

FIG. 11. (a) Raw data of S_{inc}^{el} in absolute units as observed in the ⟨001⟩ direction at $T=573$ K (solid symbols, measured with $k_f=2.662$ Å^{-1}; open symbols, measured with $k_f=4.4$ Å^{-1}). The solid line shows the calculated coherent elastic neutron scattering due to the proton-induced host lattice distortions (Ref. 5). (b) Corrected data S_{inc}^{el} plotted on a logarithmic scale vs Q^2. The dashed lines indicate two possible straight sections associated with a Debye-Waller-like behavior.

was calculated numerically using a two-force Kanzaki model [the solid line in Fig. 11(a) shows the dimensionless quantity $S^{el}_{coh}(\mathbf{Q})/(b_c^{Nb})^2$] and subtracted from the data. For a more detailed description of this calculation, see Ref. 5; note here that this data correction is only possible when the incoherent diffuse scattering is determined very accurately on an absolute scale. Consider again Fig. 11(a): If, as hitherto assumed, the quasielastic intensity could be described by a Debye-Waller factor only, the Q dependence of $S^{el}_{inc}(\mathbf{Q})$ should be Gaussian [$\sim \exp(-Q^2\langle u^2_H\rangle)$]. Mere inspection by eye already tells one that this is obviously not the case, since $S^{el}_{inc}(\mathbf{Q})$ is far too high for large momentum transfer Q. When $\ln[S^{el}_{inc}(\mathbf{Q})]$ is plotted versus Q^2 ("Debye-Waller factor plot"), this shows up in an anomalously steep slope at small values of Q [Fig. 11(b)], a phenomenon which has also been observed previously (however, on a much more limited Q range) and was called the "anomalous Debye-Waller factor".[23] Apparently, $S^{el}_{inc}(\mathbf{Q})$ is of a more complicated nature; thus, we have to proceed here in a different way: To account for the vibratory motion of the interstitial hydrogen as caused by the band and localized modes, we have to determine the proper Debye-Waller factor. The mean-square displacement is[20]

$$\langle u^2_H\rangle = \langle u^2_H\rangle_{loc} + \langle u^2_H\rangle_{band} = \langle u^2_H\rangle_{loc} + g\langle u^2_{Nb}\rangle \,, \quad (33)$$

where $\langle u^2_H\rangle_{band}$ and $\langle u^2_H\rangle_{loc}$ are the mean-square displacement due to the band modes and localized modes, respectively. The coupling parameter g is expected to be slightly greater than 1. Whenever the structure factor $S^{el*}_{inc}(\mathbf{Q})$ oscillates in Q (as discussed above), the experimental determination of the Debye-Waller factor cannot be performed as indicated in Fig. 11(b). However, quite generally, the Debye-Waller factor can be deduced from the ratio of intensities at Q values which are equivalent in the relevant reciprocal lattice [in our case the reciprocal lattice of the tetrahedral sites (see Fig. 7)]. Thus, when

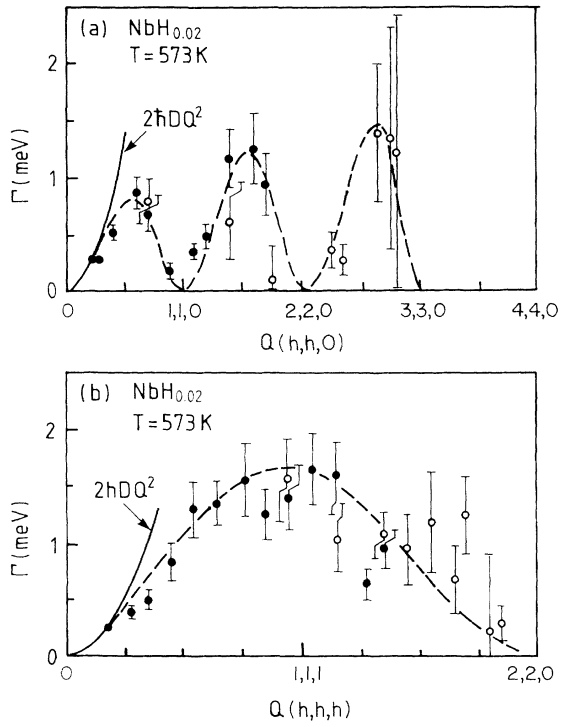

FIG. 12. Lorentzian half-widths obtained from fits of the quasielastic spectra (solid symbols, measured with $k_f = 2.662$ Å^{-1}; open symbols, measured with $k_f = 4.4$ Å^{-1}) (a) along the [110] direction and (b) along the [111] direction. The dashed line indicates the periodicity expected for tetrahedral interstitial diffusion. The long-ranged diffusion parabola at small Q is shown.

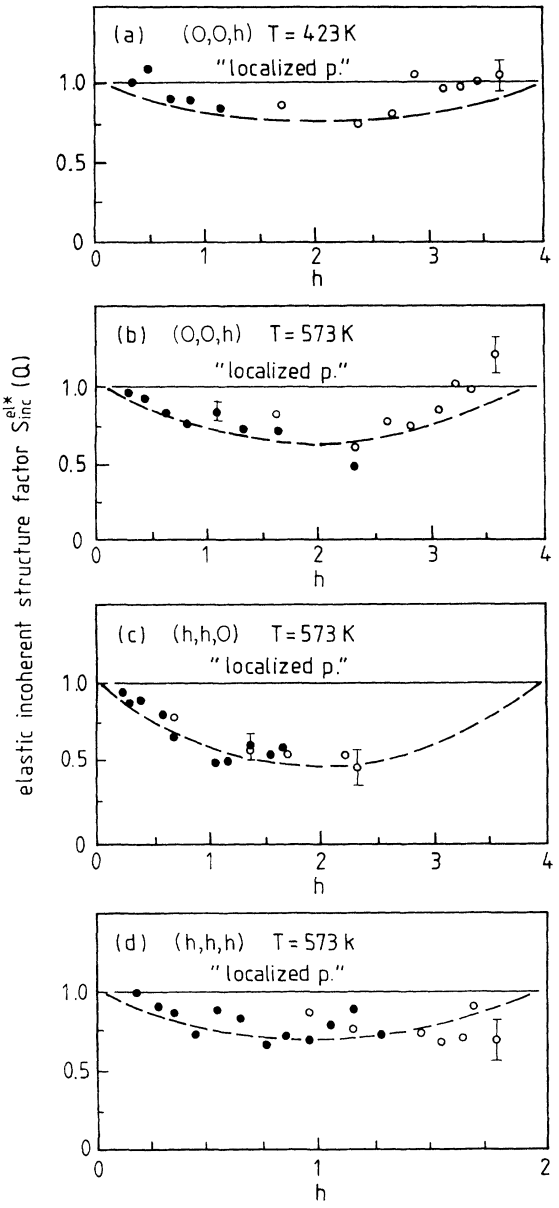

FIG. 13. Final experimental results for S^{el*}_{inc} (a), (b) in the [001] direction for two different temperatures $T = 423$ and 573 K, (c) in the [110] direction at $T = 573$ K, and (d) in the [111] direction at $T = 573$ K (solid symbols, measured with $k_f = 2.662$ Å^{-1}; open symbols, measured with $k_f = 4.4$ Å^{-1}). The solid horizontal line shows the expected behavior for a localized proton. The dashed curves are guide for the eyes.

we divide the observed $S_{\rm inc}^{\rm el}(\mathbf{Q})$ by the *correct* Debye-Waller factor $\exp(-Q^2\langle u_{\rm H}^2\rangle)$, the so-obtained quantity $S_{\rm inc}^{\rm el*}(\mathbf{Q}) \equiv S_{\rm inc}^{\rm el}(\mathbf{Q})/\exp(-Q^2\langle u_{\rm H}^2\rangle)$ must become symmetric in the reciprocal interstitial lattice. This argument holds independently of the applied diffusion model; the only underlying assumption is that the diffusion can be described by jumps between tetrahedral sites. It turns out that the quantity $S_{\rm inc}^{\rm el*}(\mathbf{Q})$ can be rendered symmetric in all measured directions of $\mathbf{Q}$ and at all temperatures when the coupling parameter g in Eq. (33) is chosen to be $g_{\rm expt}=1.35\pm0.10$. This corresponds to $\langle u_{\rm H}^2\rangle=0.031$ Å^2 at 573 K, which is a quite reasonable value.[20]

Figures 13(a)–13(d) show $S_{\rm inc}^{\rm el*}(\mathbf{Q})$ for the ⟨001⟩ direction at two different temperatures and for the ⟨110⟩, and ⟨111⟩ directions at 423 K. If there were no other mechanisms of motion than long-range diffusion and vibrations, these calibrated intensities should be constant in Q and equal to 1, in strong contrast with our observation. Most interestingly, the measured behavior of the "proton form factor" is very close to the theoretical prediction from the rapid local-diffusion model [Fig. 7(a)]; thus our conjecture is that the observed deviation of $S_{\rm inc}^{\rm el*}(\mathbf{Q})$ from unity is due to a rapid-diffusion mechanism of the proton that is significantly faster than the long-range diffusion. Since we still observe an elastic line (which is, of course, broadened by the conventional jumping contributing to the long-ranged diffusion), we further conclude that this rapid motion must be limited in space. We observe that $S_{\rm inc}^{\rm el*}(\mathbf{Q})$ depends on the direction in reciprocal space (Fig. 13), as well as on the temperature. In the ⟨001⟩ direction, this feature is very pronounced [Fig. 13(b)], while in the ⟨111⟩ direction the deviation from unity is less pronounced, an observation which may be understood by inspection of Fig. 14, which shows $S_{\rm inc}^{\rm el*}(\mathbf{Q})$ associated with the $3T$ configuration in the three main crystallographic directions: The incoherent structure factor displays oscillations which are smaller in the ⟨111⟩ direction than in the other high-symmetry directions. Finally, the observed temperature dependence implies a thermal activation of the rapid local diffusion.

We conclude from this experimental study that the deviation of $S_{\rm inc}^{\rm el}(\mathbf{Q})$ from the Debye-Waller factor behavior implies a *non-Gaussian distribution* of the proton on a time scale which is much shorter than 10^{-12} s (as given by the long-range diffusion mechanism). The periodicity measured in the ⟨001⟩ direction indicates a distribution of the proton involving several tetrahedral interstices. From the sum rule for incoherent scattering [Eq. (27)] and the deviation of $S_{\rm inc}^{\rm el*}(\mathbf{Q})$ from unity, it follows that there have to be inelastic contributions in the incoherent spectrum. From the temperature dependence of $S_{\rm inc}^{\rm el*}(\mathbf{Q})$, we follow that the rapid local diffusion must be thermally activated, an experimental fact which is certainly crucial in finding the underlying microscopic diffusion mechanism (we come to this later in the final remarks).

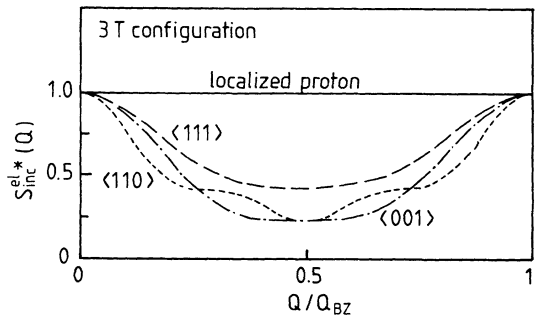

FIG. 14. $S_{\rm inc}^{\rm el*}$ associated with the $3T$ configuration for Q/Q_{BZ} in the main three crystallographic directions. Q_{BZ} is (0,0,4) in the [001] direction, (4,4,0) in the [110] direction, and (2,2,2) in the [111] direction (see also Fig. 9).

V. MEASUREMENT OF THE COHERENT QUASIELASTIC SCATTERING FROM NbD_x

The presented theory of diffuse scattering from time-dependent lattice distortions makes some remarkable predictions regarding the properties of the coherent diffuse neutron-scattering cross section. When the local mobility of the defect is sufficiently high, the noncubic long-ranged displacement components [which are, to remind the reader, coupled to the eigenvalues $\Gamma_{2,3,\ldots}=O(\nu_{\rm loc}^*)$] eventually disappear. On the other hand, coherent diffuse neutron scattering from the cubic long-ranged components of host-lattice distortions is predicted to exhibit a quasielastic width Γ_1 associated with the long-ranged diffusion process. (Note again that $\Gamma_1=0$ in the absence of long-ranged diffusion.) We have subjected this conjecture to a critical experimental test.

We have performed a neutron-scattering study of this "Huang linewidth" Γ_1 in a $NbD_{0.1}$ single crystal. The preparation of the Nb single crystal has been similar to the one described above. In order to assure, however, that the system always remained in the α phase (where the defects are randomly distributed), the D doping of the Nb single crystal was done this time *in situ* in a special furnace which kept the sample temperature always above the associated phase-transition temperature. The neutron-scattering experiments have been performed at $T=220$ °C using the triple-axis neutron spectrometers IN12 and D10 (ILL, Grenoble). Both experiments produced essentially the same results; in the following we describe the D10 experiment. With an incident wave vector $k_i=2.665$ Å^{-1}, the PG(004) reflection for the monochromator and analyzer and 10-min collimators we achieved a relatively high-energy resolution of $\Delta E=0.213$ meV at $E=0$. We measured the energy distribution of Huang diffuse neutron scattering around the (200) Bragg reflection along $\mathbf{q}=q_0(1,0,0)$, i.e., in the so-called "radial" direction, which is sensitive to cubic components in the long-ranged displacement field.[9] Typical examples of the observed scattering distribution are shown in Fig. 15 for (a) $q_0=0.1$ and (b) $q_0=0.3$. The deduced intrinsic energy widths Γ_1 of the Huang diffuse scattering increase, as expected from the above theory, with q_0 (Fig. 16). The solid line is theoretical values of Γ_1 assuming uncorrelated nearest-neighbor jumps of the defect ("Chudley-Elliott model"); the dashed line is predicted from the so called two-state model introduced by Lottner *et al.*,[3] which has

been extended by Dosch, Peisl, and Dorner[5] by including delocalized local lattice distortions. Even though the large error bars in Γ_1^{exp} do not allow one to distinguish between the models, we can conclude that "cubic" Huang diffuse scattering exhibits, as predicted in Sec. II, a linewidth which depends upon q_0^2 and ranges an energy which is related to the long-ranged diffusion process.

The conclusions drawn from this study also have a subtle, but quite interesting, consequence for the interpretation of the coherent quasielastic neutron scattering reported by Dosch, Peisl, and Dorner.[5] In Fig. 17 we show again one of their results, the coherent elastic diffuse scattering from $NbD_{0.017}$ at room temperature as a function of the momentum transfer Q whose range has been chosen such that the scattering is most sensitive to the local defect neighborhood. Furthermore, the energy resolution of this experiment has been coarsened to $\Delta E = 3.8$ meV in order to assure a reliable integration over the quasielastic broadening as induced by the mobility of the defect, which was still assumed at this time to be governed by a room-temperature jumping frequency around $\nu_{LR} \simeq 10^{12}$ s^{-1}. Scattering-theory then tells you

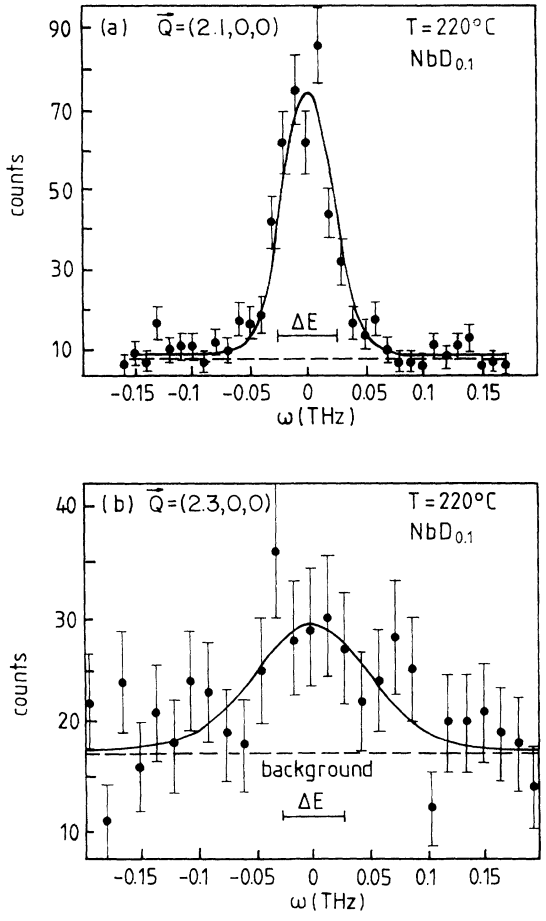

FIG. 15. Energy distribution of the neutron Huang diffuse scattering from $NbD_{0.1}$ at $T = 220$°C around the (200) Bragg reflection at $\mathbf{q} = q_0(1,0,0)$ for (a) $q_0 = 0.1$ and (b) $q_0 = 0.3$. The solid lines are convoluted Lorentzian fits.

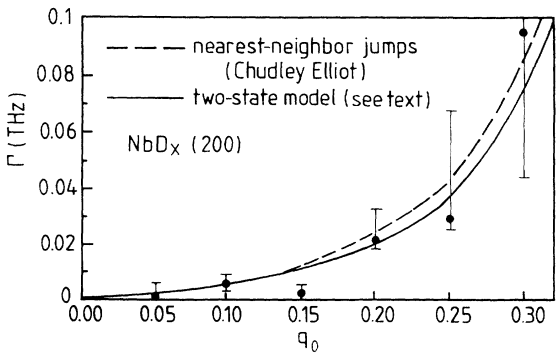

FIG. 16. Huang energy width vs q_0 as observed in the (200) Brillouin zone. The solid line assumes nearest-neighbor jumps, and the dashed line follows from the two-state model (see text).

that the mobile proton (or here deuteron) should be considered localized, in this case, on a tetrahedral site. The dashed line has been calculated by Dosch, Peisl, and Dorner[5] for a localized defect within a local distortion field, which, however, appears extended over three adjacent tetrahedral sites [for comparison, we also show the wrong prediction (dotted line) of the "$\epsilon_{12} = 0.23$" model mentioned above]. Since we have a strong experimental evidence now that the local mobility of the defect is roughly two orders of magnitude higher than assumed previously, the proper calculation of the coherent scattering shown in Fig. 17 has to account for a delocalized defect. We thus recalculated this scattering cross section accordingly and obtained the solid line which indeed reproduces the observed structure of the diffuse scattering much better than the previous calculation.

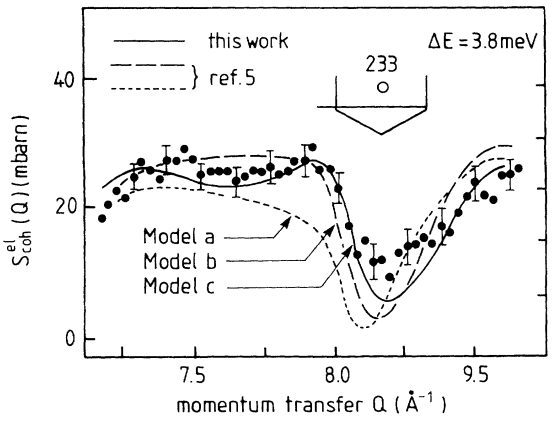

FIG. 17. Coherent quasielastic neutron scattering from $NbD_{0.017}$ at room temperature (Ref. 5). The dashed line is the best fit assuming the defect localized with a distorted region over three neighboring tetrahedral sites (Ref. 5), and the dotted line follows from a *cubic* frozen force dipole moment ("$\epsilon_{12} = 0.23$"). The solid line is obtained when the same local distortions are used which give the dashed line, however, assuming in addition that the defect appears delocalized over three adjacent tetrahedral sites within the energy resolution of the experiment.

VI. FINAL REMARKS

At first sight the proposed local-diffusion mechanism on a time scale of $\tau = \nu_{\text{loc}}^{*-1} \simeq 10^{-13}-10^{-14}$ s may be quite surprising, or even disturbing. We ourselves have been reluctant for quite a long time to accept it, since one would think, e.g., that in the whole body of incoherent quasielastic-scattering studies[2] one of the linewidths $\{\Gamma_2, \Gamma_3, \text{etc.}\}$ associated with the proposed rapid local diffusion must have been detected somehow. We then analyzed various experimental conditions carefully and arrived at the following conclusion: The energy resolution in all these studies was (of course) adjusted to the small width Γ_1 of the long-ranged diffusion mechanism (note that Γ_1 is not affected by any local diffusion); consequently, the expected large widths $\Gamma_{2,3,\ldots}$ (typically some 10 meV) would merely appear as a very broad scattering background. In an experiment[24] performed with hot neutrons at the triple-axis spectrometer IN1 (ILL), we attempted to pick up some inelastic-scattering signals which could be related to the local rapid-diffusion mechanism. The experiment on a $NbH_{0.02}$ single crystal has been performed with a very coarse energy resolution of $\Delta E = 4.7$ meV at $E = 0$ at two temperatures $T = 300$ and 580 K. Unfortunately, it turned out that the investigated energy range $E = 0-60$ meV is so strongly dominated by inelastic scattering from H-band modes, multiphonon processes, and, in particular, unidentified spurious diffuse scattering from the monochromator and analyzer crystals that a reliable measurement of the expected inelastic signal was impossible. At this point we should also note that the actual energy distribution of the local diffusion-mediated inelastic scattering is very uncertain at the present stage, since it depends crucially upon the microscopic details of the actual diffusion mechanism, which are not known. In principle, this rapid local-diffusion mechanism may be brought about by thermally activated jumps over a (so far unknown) potential barrier within the configuration shown in Fig. 4(b) or by a localized tunneling process through these (quasi)static potential barriers within the configuration. The associated incoherent neutron-scattering function exhibits broad Lorentzian spectra (with widths $\Gamma_{2,3,\ldots}$) in the first case and energetically discrete excitations in the latter. In the case, however, where the tunneling frequency is comparable to a typical phonon frequency, the potential barrier is perturbed during the tunneling process by the lattice vibrations. Therefore those tunneling excitation which are in the energy regime of lattice phonons are expected to be completely blurred in energy.

Despite these uncertainties concerning the inelastic channels of the local diffusion, the experimental evidence for it has become so striking that one is forced to reconsider one's old conceptions concerning the diffusion mechanism of interstitial hydrogen in bcc metals. In this study, we presented theoretical arguments and additional experimental evidence that such a dynamics may be present in NbH_x and NbD_x, at least at elevated temperatures. Many of the long-standing puzzling properties of interstitial hydrogen in bcc metals that have been in the literature no longer appear as puzzling in the light of a rapid local-diffusion mechanism. Some of these arguments are already found in Ref. 5. We add here another phenomenon which even allows an independent estimate of the local jumping frequency ν_{loc}^{*}: Richter and Shapiro[8] report measurements of the energy width ΔE_{loc} of the localized vibrations in $NbH_{0.82}$. While ΔE_{loc} is negligibly small at $T = 300$ K, where the system is in the ordered β phase which exhibits long-range order among the proton and, accordingly, a significantly reduced proton mobility, unusually large values of ΔE_{loc} are observed at $T = 433$ K when the system is in the disordered α' phase, which allows a high mobility of the protons. From the uncertainty relation $\Delta E\, \Delta\tau \simeq \hbar$, we deduce a lifetime of the local modes of $\Delta\tau \simeq 3.5 \times 10^{-14}$ s, which is surprisingly close to the time scale which we deduced from the criterion that the noncubic long-ranged displacement components disappear.

ACKNOWLEDGMENTS

We are indebted to Bruno Dorner, whose experimental expertise was an indispensable help during our experimental runs at the Institut Laue-Langevin. We thank J. Bierfeld for the H doping of the crystals, Helmut Schober, Claude Zeyen, and Eberhard Burkel for kind experimental assistance, and Klaus Kehr for inspiring discussions. We are grateful to the Institut Laue-Langevin for the hospitality during our stays at the high flux reactor. This work was supported by the Bundesministerium für Forschung und Technologie.

---

*Present address: Universität Mainz, Institut für Physik, D-6500 Mainz 1, Germany.

[1]For a review, see T. Springer, *Quasi-Elastic Scattering of Neutrons for the Investigation of Diffusive Motion in Solids and Liquids*, Vol. 64 of *Springer Tracts in Modern Physics* (Springer-Verlag, Berlin, 1972); *Hydrogen in Metals I*, edited by G. Alefeld and J. Völkl, Vol. 28 of *Topics in Applied Physics* (Springer, Berlin, 1978).

[2]W. Gissler, G. Alefeld, and T. Springer, J. Phys. Chem. Solids **31**, 2361 (1970); H. K. Birnbaum and C. P. Flynn, Phys. Rev. Lett. **37**, 25 (1976); K. W. Kehr, in *Hydrogen in Metals I*, Ref. 1; R. M. Cotts, in *Hydrogen in Metals I*, Ref. 1.

[3]V. Lottner, J. W. Haus, A. Heim, and K. W. Kehr, J. Phys. Chem. Solids **40**, 557 (1979).

[4]H. Dosch and J. Peisl, Phys. Rev. Lett. **56**, 1385 (1986).

[5]H. Dosch, J. Peisl, and B. Dorner, Phys. Rev. B **35**, 3069 (1987).

[6]G. S. Bauer, E. Seitz, H. Horner, and W. Schmatz, Solid State Commun. **17**, 161 (1975).

[7]H. Metzger, J. Peisl, and J. Wanagel, J. Phys. F **6**, 2195 (1976).

[8]D. Richter and S. M. Shapiro, Phys. Rev. B **22**, 599 (1980).
[9]H. Trinkaus, Phys. Status Solidi B **51**, 307 (1972).
[10]P. H. Dederichs, J. Phys. F **3**, 471 (1973).
[11]H. Kanzaki, J. Phys. Chem. Solids **2**, 107 (1957).
[12]G. Leibfried and N. Breuer, *Point Defects in Metals I,* Vol. 81 of *Springer Tracts in Modern Physics* (Springer, Berlin, 1976).
[13]For a localized diffusion ($\Gamma_1=0$), the relation $\sum_i U_{i1}\underline{P}_i=\sum_i \underline{P}_i$ is exact.
[14]M. J. Gillan and D. Wolf, Phys. Rev. Lett. **55**, 1299 (1965).
[15]R. I. Sharp, J. Phys. C **2**, 421 (1969); V. K. Tewary, J. Phys. F **3**, 1515 (1973); in the actual calculation we used the elastic constants associated with $NbD_{0.1}$ at $T=500$ K: F. M. Mazzolai and H. K. Birnbaum, J. Phys. F **15**, 507 (1985).
[16]D. Emin, Phys. Rev. Lett. **25**, 1751 (1970); Phys. Rev. B **3**, 1321 (1971).
[17]In the derivation of Eq. (17), we used the fact that $\int S_{\rm coh}(\mathbf{Q},\omega)\omega^2 d\omega=Nk_BT/m_0$ holds, independent of the defect concentration *("f-sum rule");* see, e.g., D. Forster, *Hydrodynamic Fluctuations, Broken Symmetry and Correlation Functions,* Vol. 47 of *Frontiers in Physics* (Benjamin, Reading, 1975).
[18]For an introduction to incoherent neutron scattering, see S. W. Lovesey, *Theory of Neutron Scattering from Condensed Matter* (Clarendon, Oxford, 1987), Vol. 1.
[19]Since we are interested in the following only in the elastic part of the scattering function, we may treat the Heisenberg operators $\mathbf{r}_j$ as c-numbers; thereby, we implicitly ignore the principle of detailed balance, $S(\mathbf{Q},\omega)=\exp(\hbar\omega/kT_B)S(\mathbf{Q},-\omega)$. However, the principle of detailed balance can approximately be accounted for by an appropriate factor which ensures that $S(\mathbf{Q},\omega)/S(\mathbf{Q},-\omega)=\exp(\hbar\omega/k_BT)$; see P. Schofield, Phys. Rev. Lett. **4**, 239 (1960).
[20]V. Lottner and H. R. Schober, Phys. Rev. Lett. **42**, 1162 (1979); V. Lottner, A. Heim, and T. Springer, Z. Phys. B **32**, 157 (1979).
[21]The H doping of the crystal has been performed by J. Bierfeld and H. Wenzl.
[22]Note that the observed line is strictly speaking a superposition of several Lorentzians according to a diffusion on a non-Bravais lattice. A detailed test of some spectra, however, showed that the integrated intensity is rather insensitive to these details.
[23]N. Wakabayashi, B. Alefeld, K. W. Kehr, and T. Springer, Solid State Commun. **15**, 503 (1974).
[24]H. Dosch, P. Wiethoff, F. Schmid, and B. Dorner (unpublished results).